Materials Research Express

Magnetocaloric effect and electrical properties of (0.95)La_{0.45}Nd_{0.25}Sr_{0.3}MnO₃/ (0.05)CuO composites.

To cite this article before publication: lahcen fkhar *et al* 2020 *Mater. Res. Express* in press https://doi.org/10.1088/2053-1591/ab9c62

Magnetocaloric effect and electrical properties of $(0.95)La_{0.45}Nd_{0.25}Sr_{0.3}MnO_3/ (0.05)CuO$ composites.

L.Fkhar[1, 2,*], K. El Maalam[2], M. Hamedoun[2], A. El Kenz[3], A. Benyoussef[2, 3,4], , P. Lachkar[5], E.-K.Hlil[5], A. Mahmoud[6], F. Boschini[6], M. Ait Ali[1], O. Mounkachi[3]

[1]*Coordination Chemistry Laboratory, Cadi Ayyad University, Faculty of sciences Semlalia (UCA-FSSM), B.P. 2390 - 40000 Marrakech, Morocco,*

[2]*Materials and Nanomaterials Center, MAScIR Foundation, B.P. 10100-Rabat, Morocco.*

[3]*Laboratory of Condensed Matter and Interdisciplinary Sciences (LaMCScI) , B.P. 1014, Faculty of science, Mohammed V University, Rabat, Morocco,*

[4]*Hassan II Academy of Science and Technology, Rabat, Morocco,*

[5]*Institut Néel, CNRS-UJF, B.P. 166, 38042 Grenoble Cedex, France*

[6]*GREENMAT, CESAM, Institute of Chemistry B6, University of Liege, 4000 Liège, Belgium*

E-mail fkhar.lahcen@gmail.com

Abstract:

In this work, the structural, magnetic and magnetocaloric properties of $0.95La_{0.45}Nd_{0.25}Sr_{0.3}MnO_3/0.05CuO$ composites materials were investigated. The samples have been synthesized by solid-state reaction route. The XRD patterns of composites powders show the presence of both perovskite $La_{0.45}Nd_{0.25}Sr_{0.3}MnO_3$ and monoclinic Tenorite CuO materials. The microstructural characterization performed using Scanning Electron Microscope shows that copper oxide nanostructure is located in the grains boundaries after pressing. According to the isothermal magnetization measurements around the Curie temperature, the maximum isothermal magnetic entropy change is calculated to be 4.128 J/(Kg.K) at 5T for the pellet with an interesting enhancement compared to the powder sample 2.7 J/(Kg.K). The relative cooling power is about 212.8 J/Kg. Resistivity measurements under different magnetic fields were performed in order to investigate the magnetoresistance properties. The obtained magnetocaloric properties show that $0.95La_{0.45}Nd_{0.25}Sr_{0.3}MnO_3/0.05CuO$ composite was an attractive candidate material for magnetic refrigeration application. About magnetoresistance properties the (% MR) is found to be 32.78 % around 320 K under a magnetic field of 5 T.

Keys words:

Magnetocaloric Effect, Perovskite Manganite, Magnetic entropy change, electrical properties.

I. Introduction:

The magnetic refrigeration (MR) is a promising alternative approach for the cooling product, compared to conventional refrigeration thanks to its important advantages such as environmentally friendly and energy-efficient technology [1–3]. This technology is based essentially on the magnetocaloric effect (MCE), which is an intrinsic property of the magnetic materials that are heating up when they are posed in an extern magnetic field and cooled when they are took-out [4,5]. Recently magnetocaloric effect has attracted interest in several domains of applications such as domestic refrigeration,[6] industrial refrigeration markets [7], catalysis [8] and medicine [9]. The first application of magnetic refrigeration in low temperature was reported by (Giuaque 1927) using the gadolinium sulfate as magnetocaloric materials [10]. The discovery of giant magnetocaloric effect by pycharsky (1997) is the main scientific event that leads in researches to the application of magnetic refrigeration at room temperature [1]. The two major parameters for the application in magnetic refrigeration are the isothermal entropy change ΔS which is proportional to the cooling power of refrigerators, and the adiabatic temperature change ΔT_{ad} that contributes largely to the enhancement of the efficiency of an active magnetic regenerator cycle [7]. Several important published works were contributed to fulfill and meet the increasing demands and needs by developing new magnetocaloric materials with a various category such as Gd, GdGeSi series [11–14], LaFeSi family [15–17], husler intermetallic [5,18,19], and the oxide ferrite and perovskite types [20–25]. The low cost and the good chemical stability represent the two essential reasons for our choice of the perovskite type materials with the general formula ABO_3 [26]. Depending on the type and the overcrowding of the A cations in the vacancy site: the system migrates from the cubic to orthorhombic or rhombohedra structure [27]. In addition to the magnetocaloric effect, perovskite materials are applied in several technological applications such as thermoelectric in the case of titanates perovskite [28]. Cerates and zirconates have high proton conductivity, which give them an important place in hydrogen fuel cell and sensors applications [29,30]. As for manganite perovskite, very good magnetic properties caused the reservation of this family of perovskite to magneto-resistance and magnetocaloric effect [31–33]. The perovskite type ABO_3 materials could be synthesized by all usual ceramic reaction methods like solid state reaction [34], solution technologies including sol- gel and co-precipitation and others [35], hydrothermal, hydrothermal-electrochemical by using an electric field, Microwave synthesis and Physical vapor

deposition (PVD) methods – laser ablation or Molecular beam epitaxy (MBE) for thin films [36]. Recently, we have reported the synthesis and magnetocaloric properties of $(La_{0.45}Nd_{0.25})Sr_{0.3}MnO_3$ (LNSMO)-based composites [37,38]. We have shown that the 0.95LNSMO/0.05CuO samples with micro particles of copper oxide, for a magnetic field changing from 0 to 1.5 T, the corresponding isothermal entropy change was found to be 2.55 J/kg K. In the course of our studies on magnetocaloric properties of LNSMO composites and following our objective for their enhancement, we focused our efforts on the synthesis of polycrystalline 0.95LNSMO/0.05CuO composites using nanoparticles of copper oxide instead of the micro particles. We have then study the effect of the size of the secondary phase (CuO) on the magnetic and magnetocaloric properties of the composite. In addition, we report the electrical properties of our composite such as resistivity and heat capacity. Our results show that the magnetic entropy change calculated with the isothermal data increases from 2.69 J/(Kg.K) for the powder to 4.12 J/(Kg.K) in the case of pellet.

II. Experimental details :

Polycrystalline 0.95LNSMO/0.05CuO composites were prepared by the conventional solid-state reaction method. Lanthanum oxide La_2O_3 (99%, Sigma-Aldrich), Neodymium oxide Nd_2O_3 (99%, Alfa Aesar), strontium oxide SrO (99.5%, Alfa Aesar), manganese III oxide Mn_2O_3 (98%, Alfa Aesar), manganese IV oxide MnO_2 (98%, Alfa Aesar) and copper oxide CuO nanostructure (US-Nano) were used as precursors. Firstly, the perovskite LNSMO material was prepared. Stoichiometric proportions of La_2O_3, Nd_2O_3, SrO, Mn_2O_3 and MnO_2 were ground in an agate mortar, then preheated at 1173 K for 8 h under air with intermediate grinding. The preparation process was been achieved by annealing the sample at 1473 K for 12 h under air. The polycrystalline composites LNSMO/0.05CuO were been obtained by mixing the copper oxide (CuO) with the calcined LNSMO in a 5% weight ratio. The resulting product has been subjected to a heat treatment at 1473 K for 2 h under air. In the case of pellet, the resulting product was thoroughly mixed with PEG in water for 2 hours, then the powder was dried, pressed and calcined at 1473 K for 2 h. The structural characterization was made by X-ray powder diffraction using Model D8 Discover Bruker AXS) with Cu Kα radiation (λ_{Cu} =1.5407 Å). Scanning Electron Microscope (FEI Quanta FEG 450) equipped with Energy Dispersive X-ray (EDX) detector. The magnetic and magnetocaloric properties were performed using Magnetic Properties Measurement System (MPMS-7XL), with a Quantum

Design XL-SQUID magnetometer. The electrical properties and the specific heat properties were created using Quantum Design PPMS-9.

III. Results and discussions:

1- Structural and morphological characterization:

Figure 1 shows the X-ray diffraction patterns of LNSMO/ CuO powder and pellet. According to the XRD data, the co-existence of two different phases showed, which confirms the formation of the LNSMO/ CuO composite materials. The rhombohedra phase of LNSMO perovskite with the space group R-3c (167) is detected which can be indexed according to PDF NO 01-082-1152. While two clear peaks at (2Θ = 35.43 and 38.47) are attributed to CuO phase. The low intensity of the CuO peak is due to the low content (5%) of the CuO in the composite materials. No other phase is detected implies that no chemical reaction between the perovskite and copper oxide. In order to study the microstructure and the morphology of our samples, the Scanning Electron Microscopy (SEM) has been used to observe the surface of the samples. Figure 2 (a) shows the SEM images of the studied powders, we can see clearly that the particles have two different sizes. Also, we can separate two different chemical compositions; one corresponds to the particles of the perovskite material with the average size of 1 µm and the second with medium-size particles of 300 nm corresponding to the particles of copper oxide which are distributed on the surface of the grains and in the grains boundaries. Figure 2 (b) presents the micrograph of the pellet. The chemical composition and EDS analyses indicate that the copper oxide occupies majorly the grains boundaries due to the pressure effect [38].

2- Magnetic characterization:

Figure 3 (a) illustrates the magnetization as a function of the temperature from 200K to 400K of the powder and the pellet samples under a magnetic field of 500 Oe. Both materials exhibit a magnetic transition from ferromagnetic to paramagnetic order. The magnetic moment at a low temperature of the pellet is found to be 41.8 emu/g, which is the double of the obtained value for the powder perovskite (20.47 emu/g). Figure 3 (b) shows the temperature depending on the derivative of magnetization (dM/dT) in the temperature range of 150 K and 400 K. T_C values determined from the flexion points in $M(T)$ curves are about 336.16 and 321.01 K for powder and pellet respectively. The Tc of the pellet decreases with 15 K, which is in good agreement with the study of the effect of pressure on the Tc reported by Masahiro shikano [39],

also the copper oxide, that occupies largely the grains boundaries in the pellet, is characterized by an antiferromagnetic order with Néel transition at 230 K [40]. The isothermal magnetization as a function of a magnetic field up to 5 tesla and at different temperatures from 200 K to 400 K for the powder and pellet are shown in Figure 4 (a) and (b), respectively. We can clearly distinct two regions: one of the ferromagnetic phase characterized by non-linear comportment, with a tendency of saturation at higher fields, this region is connected by the transition temperature with the second region, which exhibits a linear behavior when the temperature is above of Tc. This result confirms the paramagnetic phase in this region. The Banerjee criterion is frequently recommended to determine the nature of the magnetic transition. It is based on H/M depending on M^2; when the slope is negative the magnetic transition is of first order, on the other hand when the slope is positive the magnetic transition becomes of second order [41]. Figure 5 (a) and (b) show the Arrott plots (M^2 as function H/M) for the LNSMO/CuO powder and pellet samples, respectively. From figure 5, the slope of the Arrott plots is positive which corresponds to the second order transition.

3- Magnetocaloric characterization:

The magnetic entropy change ΔS_M is the most recommended parameter to evaluate the magnetocaloric effect of magnetic materials. It can be calculated by integrating Maxwell's relation using the isothermal magnetization depending on the magnetic field as data [42]:

$$\Delta S_m = \int_0^H \left(\frac{\partial M}{\partial T}\right)_H dH \qquad (1)$$

Figure 6(a) and (b) represent the magnetic entropy change as a function of temperature for the powder and the pellet under the different fields, respectively. From Figure 6, the magnetic entropy has a maximum around the transition temperature and decreases when moving away from the transition temperature to right and left. In the case of the pellet, the operating temperature decreases. The value of the maximum entropy change is found to be 2.69 J/(Kg.K). and 4.12 J/(Kg.K). For the powder and the pellet, this increase between the powder and the pellet may be due to the external pressure. These values are in the same range compared with other manganite or manganite composites [43–47], some intermetallic materials [48,49], and they are very large compared with other oxides [50,51].

The relative cooling power (RCP) is an important parameter to evaluate the efficiency of the magnetocaloric material for magnetic refrigeration. The RCP is giving by the following formula:

$$RCP = |\Delta S_{max}| \times \delta T_{FWHM} \quad (2)$$

Where ΔS_{max} is the maximum magnetic entropy change and δT_{FWHM} is the full width at half maximum of the magnetic entropy change. Figure 7 (a) regroups the values of ΔS_{max} under various magnetic field from 1 to 5 tesla for both powder and pellet samples, ΔS_{max} increases linearly with increasing the magnetic field. We observed that the obtained values for pellet are superior compared to the powder sample.

Figure 7 (b) shows the relative cooling power RCP as a function of the magnetic field from 1 to 5 T. The obtained values show a linear dependence on the magnetic field with a noticeable decrease from 296.92 J/Kg for the powder to 208.44 J/Kg for the pellet under 5 tesla. That is due essentially to the operating temperature caused by the application of external pressure in the pellet.

4- Electrical properties:

Figure 8 presents the electrical resistivity of the pellet as a function of the temperature from 10 to 350 K without and under different magnetic fields from 1 to 5 T. it is found that our pellet sample exhibits a metal-insulator transition in the range of 300 K and 315 K. Moreover, we observed that the resistivity is inversely proportional to the applied magnetic field, which can be due to the influence of the magnetic field on the delocalization of the charge carriers, causing the increase of the electrical conductivity, which is related to the diminution of the electrical resistivity [52,53].

From the electrical resistivity data, we calculated the magnetoresistance using the following formula:

$$\text{MR}\,(\%) = \frac{R_0 - R_H}{R_0} \times 100 \quad (3)$$

Where R_0 and R_H represent the resistivity without and under the applied magnetic field respectively. The temperature dependence of the magnetoresistance (MR) is shown in Figure 9 (a). The peak of the MR was found up to 32.78 % around 320 K for a magnetic field of 5 T. The observed value of the MR is in the same range of $La_{0.71}Sr_{0.29}MnO_3$ at low field (MR=30 %) [54]. And higher than that calculated in other simple perovskite manganite reported in the literature such as $Pr_{0.67}Sr_{0.33}MnO_3$ (MR= 30 %) [55] $La_{0.7}Sr_{0.2}Na_{0.1}MnO_3$ (MR= 25%) [56], and lower than that of $Nd_{0.6}Sr_{0.4}MnO_3$ and $La_{1-x}Ca_xMnO3$ prepared by sol gel method (MR= 99.84%) [45,57] and $La_{0.67-x}RE_xCa_{0.33}MnO_3$ (RE = Nd, Sm, and Gd, x = 0.0, 0.1) [58]. In addition, as it is shown in Figure 9 (b), the maximum of the MR value of LNSMO/CuO around the transition temperature increases from 9.82% for a magnetic field of 1 T to 32.77 % for 5T, which reveals the magnetoresistance sensitivity of LNSMO/CuO composites to the external applied magnetic field.

Figure 10 presents the heat capacity of (LNSMO/CuO) in the absence and under 1 tesla of the external magnetic field. It is found that the heat capacity Cp under and without magnetic field are superposed bellow and after magnetic transition. While, in the range of the transition temperature, we observed that the peak of the heat capacity in the absence of an external magnetic field, which is related to the magnetic transition shown previously in the magnetization measurement, is higher and narrow that when applied a magnetic field of 1T. This comportment accords well with the typical characteristic of ferromagnetic materials as reported in the literature [59]

Conclusions:

In summary, $0.95La_{0.45}Nd_{0.25}Sr_{0.3}MnO_3/0.05CuO$ composites were synthesized using solid-state reaction process. The existence of two phases (rhombohedra perovskite and monoclinic of copper oxide) are confirmed by X-Ray diffraction. Copper oxide occupied the grains boundaries for the powder and pellet samples. The magnetic entropy change calculated with the isothermal data increases from 2.69 J/(Kg.K) for the powder to 4.12 J/(Kg.K) in the case of the pellet. This result indicates that the perovskite/CuO composites with a pellet design are more favorably than the powder magnetic refrigeration applications.

References

[1] Pecharsky V K and Gschneidner K A 1997 Giant magnetocaloric effect in Gd5 (Si2 Ge2) *Phys. Rev. Lett.* **78** 4494–7

[2] Hu F X, Shen B G, Sun J R, Cheng Z H, Rao G H and Zhang X X 2001 Influence of negative lattice expansion and metamagnetic transition on magnetic entropy change in the compound LaFe11.4Si1.6 *Appl. Phys. Lett.* **78** 3675–7

[3] A. Fujita, S. Fujieda, Y. Hasegawa K F 2003 Itinerant-electron metamagnetic transition and large magnetocaloric effects in La(FexSi1-x)13 compounds and their hydrides *Phys. Rev. B* **67** 104416

[4] Gschneider Jr. K A, Pecharsky V K and Tsokol A O 2005 Recent developments in magnetocaloric materials *Reports Prog. Phys.* **68** 1479–539

[5] Liu J, Gottschall T, Skokov K P, Moore J D and Gutfleisch O 2012 Giant magnetocaloric effect driven by structural transitions *Nat. Mater.* **11** 620–6

[6] Kitanovski A and Egolf P W 2009 Application of magnetic refrigeration and its assessment *J. Magn. Magn. Mater.* **321** 777–81

[7] ARIANA DE CAMPOS D, CARVALHO A G, CARON L, ADELINO A. COELHO, SERGIO GAMA, LUZELIM.DA SILVA F C G G, ADENILSON O. DOS SANTOS L P C, RANKE2 P J VON and OLIVEIRA N A DE 2006 Ambient pressure colossal magnetocaloric effect tuned by composition in Mn1−xFexAs *Nat. Mater.* **5** 802–4

[8] Hasnaoui A, Fkhar L, Nayad A, Mahmoud A, Mounkachi O, Hamedoun M, El L and Ali M A 2020 Synthesis and characterization of magnetic perovskites La 1-x Sr x MnO 3 : Green catalyst for oxidation of olefins in *Inorg. Chem. Commun.* 107892

[9] Tishin A M and Spichkin Y I 2014 Recent progress in magnetocaloric effect: Mechanisms and potential applications *Int. J. Refrig.* **37** 223–9

[10] Giauque W F 1927 A thermodynamic treatment of certain magnetic effects. A proposed method of producing temperatures considerably below 1° absolute *J. Am. Chem. Soc.* **49** 1864–70

[11] Pecharsky V K and Gschneidner K A 1997 Tunable magnetic regenerator alloys with a giant magnetocaloric effect for magnetic refrigeration from ~20 to ~290 K *Appl. Phys. Lett.* **70** 3299

[12] PECHARSKY, V. K.; GSCHNEIDNER K A 1997 Effect of alloying on the giant magnetocaloric effect of Gd5(Si2Ge2) *J. Magn. Magn. Mater.* **167** L179–84

[13] Zeng H, Zhang J, Kuang C and Yue M 2011 Magnetic entropy change in bulk nanocrystalline Gd metals *Appl. Nanosci.* **1** 51–7

[14] Dan'kov S, Tishin a., Pecharsky V and Gschneidner K 1998 Magnetic phase transitions and the magnetothermal properties of gadolinium *Phys. Rev. B* **57** 3478–90

[15] Dai Y, Xu Z, Luo Z, Han K, Zhai Q and Zheng H 2018 Phase formation kinetics, hardness and magnetocaloric effect of sub-rapidly solidified LaFe11.6Si1.4plates during isothermal annealing *J. Magn. Magn. Mater.* **454** 356–61

[16] Balli M, Fruchart D and Gignoux D 2008 The LaFe11.2Co0.7Si1.1Cx carbides for magnetic refrigeration close to room temperature *Appl. Phys. Lett.* **92** 17–20

[17] Bjørk R, Bahl C R H and Katter M 2010 Magnetocaloric properties of LaFe13−x−yCoxSiy and commercial grade Gd *J. Magn. Magn. Mater.* **322** 3882–8

[18] Aryal A, Quetz A, Pandey S, Dubenko I, Stadler S and Ali N 2017 Magnetocaloric effects and transport properties of rare-earth (R ¼ La, Pr, Sm) doped Ni50-xRxMn35Sn15 Heusler alloys *J. Alloys Compd.* **717** 254–9

[19] Cugini F, Righi L, van Eijck L, Brück E and Solzi M 2018 Cold working consequence on the magnetocaloric effect of Ni50Mn34In16 Heusler alloy *J. Alloys Compd.* **749** 211–6

[20] Gamzatov A G, Aliev A M, Yen P D H, Khanov L, Hau K X, Thanh T D, Dung N T and Yu S-C 2018 Correlation of the magnetocaloric effect and magnetostriction near the first-order phase transition in $Pr_{0.7}Sr_{0.2}Ca_{0.1}MnO_3$ manganite *J. Appl. Phys.* **124** 183902

[21] Pekała M, Pekała K, Drozd V, Fagnard J F and Vanderbemden P 2015 Effect of nanocrystalline structure on magnetocaloric effect in manganite composites (1/3)La 0.7 Ca 0.3 MnO 3 /(2/3)La 0.8 Sr 0.2 MnO 3 *J. Alloys Compd.* **629** 98–104

[22] Mikhaleva E, Eremin E, Flerov I, Kartashev A, Sablina K and Mikhashenok N 2014 Magnetization and magnetocaloric effect in La0.7Pb0.3MnO3 ceramics and 0.85(La0.7Pb0.3MnO3)-0.15(PbTiO3) composite *J. Mater. Res.* **30** 278–85

[23] M'nassri R 2017 Table-like magnetocaloric effect involving the enhancement of refrigerant capacity in (AMn0.9Ti0.1O3)1−x/(AMn0.85Ti0.15O3)x composite *Phase Transitions* **90** 687–94

[24] Vadnala S, Pal P and Asthana S 2016 Investigation of near room temperature magnetocaloric, magnetoresistance and bolometric properties of Nd0.5La0.2Sr0.3MnO3: Ag2O manganites *J. Mater. Sci. Mater. Electron.* **27** 6156–65

[25] Shlapa Y, Solopan S, Bodnaruk A, Kulyk M, Kalita V, Tykhonenko-Polishchuk Y, Tovstolytkin A and Belous A 2017 Effect of Synthesis Temperature on Structure and Magnetic Properties of (La,Nd)0.7Sr0.3MnO3 Nanoparticles *Nanoscale Res. Lett.* **12** 100

[26] Jonker G H and Van Santen J H 1950 Ferromagnetic compounds of manganese with perovskite structure *Physica* **16** 337–49

[27] Saiful Islam M 2000 Ionic transport in ABO3 perovskite oxides: a computer modelling tour *J. Mater. Chem.* **10** 1027–38

[28] Kovalevsky A V., Yaremchenko A A, Populoh S, Weidenkaff A and Frade J R 2013 Enhancement of thermoelectric performance in strontium titanate by praseodymium substitution *J. Appl. Phys.* **113** 53704

[29] Norby T and Larring Y 1997 Concentration and transport of protons in oxides *Curr. Opin. Solid State Mater. Sci.* **2** 593–9

[30] Eduardo Caetano Camilo de Souza R M 2010 Properties and Applications of Perovskite Proton Conductors *Mater. Res.* **13** 385–94

[31] Skini R, Omri A, Khlifi M, Dhahri E and Hlil E K 2014 Large magnetocaloric effect in lanthanum-deficiency manganites La 0.8-x□xCa0.2MnO3 (0.00≤x≤0.20) with a first-order magnetic phase transition *J. Magn. Magn. Mater.* **364** 5–10

[32] Thanh T D, Manh T V., Ho T A, Telegin A, Phan T L and Yu S C 2016 Universal behavior of magnetocaloric effect in a layered perovskite La 1.2 Sr 1.8 Mn 2 O 7 single crystal *Phys. B Condens. Matter* **486** 7–11

[33] Ho T A, Lim S H, Kim C M, Jung M H, Ho T O, Tho P T, Phan T L and Yu S C 2017 Magnetic and magnetocaloric properties of La0.6Ca0.4−xCexMnO3 *J. Magn. Magn. Mater.* **438** 52–9

[34] Phong P T, Bau L V., Hoan L C, Manh D H, Phuc N X and Lee I J 2015 B-site aluminum doping effect on magnetic, magnetocaloric and electro-transport properties of La0.7Sr0.3Mn1-xAlxO3 *J. Alloys Compd.* **645** 243–9

[35] Mostafa A G, Abdel-Khalek E K, Daoush W M and Moustfa S F 2008 Study of some co-precipitated manganite perovskite samples-doped iron *J. Magn. Magn. Mater.* **320** 3356–60

[36] Bhalla A S, Guo R and Roy R 2000 The perovskite structure - a review of its role in ceramic science and technology *Mater. Res. Innov.* **4** 3–26

[37] Fkhar L, Lamouri R, Mahmoud A, Boschini F, Hamedoun M, Ez-Zahraouy H, Benyoussef A, Hlil E K, Ait Ali M and Mounkachi O 2020 Enhanced Magnetic and Magnetocaloric Properties of La0.45Nd0.25Sr0.3MnO3/CuO Composite *J. Supercond. Nov. Magn.*

[38] El Maalam K, Balli M, Habouti S, Dietze M, Hamedoun M, Hlil E-K, Es-Souni M, El Kenz A, Benyoussef A and Mounkachi O 2017 Composite (La 0.45 Nd 0.25)Sr 0.3 MnO 3 /5CuO materials for magnetic refrigeration applications *J. Magn. Magn. Mater.* **449** 25–32

[39] Shikano M, Huang T-K, Inaguma Y, Itoh M and Nakamura T 1994 Pressure dependence of the magnetic transition temperature for ferromagnetic SrRuO3 *Solid*

State Commun. **90** 115–9

[40] Junodi A, Eckerti D, Trisconei G, Muller J and Reichardts W 1989 A study of the magnetic transitions in CuO : specific heat (1-330 K), magnetic susceptibility and phonon density of states A study of the magnetic transitions in CuO : specific heat (1-330 K), magnetic susceptibility and phonon density of states *J. Phys. Condens. Matter* **1** 8021–34

[41] Banerjee S K 1964 On a generalized approach to first and second order magnetic transitions *Phys. Lett.* **12** 16–7

[42] Phan M H and Yu S C 2007 Review of the magnetocaloric effect in manganite materials *J. Magn. Magn. Mater.* **308** 325–40

[43] Fkhar L, Mounkachi O, Maalam K El, Hamedoun M, Mahmoud A, Boschini F, El A and Ali M A 2019 Large Magnetic Entropy Change in Pr 2 / 3 Sr 1 / 3 MnO 3 -CuO Composite at Room Temperature *J. Supercond. Nov. Magn.* **32** 3579–3585

[44] Aoki F Y and Hayden F G 2018 Structural, magnetic and magnetocaloric properties of EuMnO3 perovskite manganite: A comprehensive MCE study *Mater. Res. Express* **5** 26107

[45] Abdel-Latif I A, Ahmed A M, Mohamed H F, Saleh S A, Paixão J A, Ziq K A, Hamad M K, Al-Nahari E G, Ghozza M and Allam S 2018 Magnetocaloric effect, electric, and dielectric properties of Nd0.6Sr0.4MnxCo1−xO3 composites *J. Magn. Magn. Mater.* **457** 126–34

[46] A R Shelke, B B Sinha, D K Shukla, D M Phase C D L and N G D 2017 Magnetocaloric effect and critical exponent analysis in electron-doped La1-xTexMnO3 compounds: A comprehensive study *Mater. Res. Express*, **4** 56102

[47] Xia H L, Yin Y Y, Dai J H, Yang J Y, Qin X M, Jin C Q and Long Y W 2015 Magnetism and magnetocaloric effect study of CaFe0.7Co0.3O3 *Mater. Res. Express* **2** 46103

[48] Ali T, Ali A, Gigli L and Khan M N 2019 Magnetocaloric effect and large refrigerant capacity at paramagnetic to ferromagnetic transition in Ni50Mn33In17 *Mater. Res.*

Express **6** 126103

[49] Singh V, Kumar R, Bag P, Rawat R and Kushwaha P 2015 Magnetocaloric effect and magnetoresistance correlation in Ge-doped Mn2Sb *Mater. Res. Express* **1** 46101

[50] Fkhar L, Mahmoud A, Boschini F, Hamedoun M, Benyoussef A, Hlil E K, Ali M A and Mounkachi O 2020 Structural, Magnetic, and Magnetocaloric Properties in Rare Earth Orthochromite (Sm, Nd, and La)CrO3 for Cooling Product *J. Supercond. Nov. Magn.* **33,** 1023–1030

[51] Maalam K El, Fkhar L, Hamedoun M, Mahmoud A, Boschini F, Hlil E K, Benyoussef A and Mounkachi O 2017 Magnetocaloric Properties of Zinc-Nickel Ferrites Around Room Temperature *J. Supercond. Nov. Magn.* **30** 1943–1947

[52] Kumar P A, Ray S, Chakraverty S and Sarma D D 2014 Magnetoresistance and electroresistance effects in Fe3O4 nanoparticle system *J. Exp. Nanosci.* **9** 391–7

[53] Ramirez A P 1997 Colossal magnetoresistance *J. Phys. Condens. Matter* **9** 8171–8199

[54] Sadhu A and Bhattacharyya S 2014 Enhanced low-field magnetoresistance in La0.71Sr 0.29MnO3 nanoparticles synthesized by the nonaqueous sol-gel route *Chem. Mater.* **26** 1702–10

[55] Abdelmoula N, Dhahri E, Fourati N and Reversat L 2004 Monovalent effects on structural , magnetic and magnetoresistance properties in doped manganite oxides **365** 25–30

[56] Choithrani R, Bhat M A and Gaur N K 2014 Influence of silver doping on the magnetoresistance and temperature coef fi cient of resistance in Pr 0 . 67 Sr 0 . 33 MnO 3 **361** 19–24

[57] Das K, Dasgupta P, Poddar A and Das I 2016 Significant enhancement of magnetoresistance with the reduction of particle size in nanometer scale *Sci. Rep.* **6** 1–12

[58] Anand Pal, Nagaraja B. S., Rachana K.J. S K V and Dhananjaya Kekuda, Ashok Rao,

Chia-Ruei Li Y-K K 2020 Enhancement of temperature coefficient of resistance (TCR) and magnetoresistance (MR) of La0.67−xRExCa0.33MnO3 (RE = Nd, Sm, and Gd, x = 0.0,0.1) system via rare-earth substitution *Mater. Res. Express* **7** 36102

[59] Lin P, Chun S H, Salamon M B, Tomioka Y, Tokura Y, Lin P, Chun S H and Salamon M B 2012 Magnetic heat capacity in lanthanum manganite single crystals **87** 5825–7

Figure captions:

Figure 1: X-ray diffraction patterns for 0.95LNSMO/0.05CuO, powder and Pellet samples.

Figure 2: SEM micrographs of particles of 0.95LNSMO/ 0.05CuO samples, (a) powder and (b) Pellet.

Figure 3: (a) Magnetization as function of temperature for 0.95LNSMO/ 0.05CuO samples powder and Pellet, (b) derivative of magnetization as function of temperature.

Figure 4: Isothermal magnetization M (H) curves at different temperatures for 0.95LNSMO/ 0.05CuO samples (a) powder (b) pellet.

Figure 5: Arrott plots (M^2 versus (H/M) curves for 0.95LNSMO/ 0.05CuO samples(a) powder (b) pellet.

Figure 6: Temperature dependence of the magnetic entropy change under different amplitudes of change in the magnetic field (ΔH=1-5T) for 0.95LNSMO/ 0.05CuO samples (a) powder (b) pellet.

Figure 7: Relative cooling power RCP depending of magnetic field and the magnetic entropy change dependence of magnetic field for 0.95LNSMO/ 0.05CuO samples (a) powder (b) pellet.

Figure 8: Resistivity as function of the temperature under different magnetic field.

Figure 9: (a) Magneto-resistance as function of temperature for different magnetic field (b) Maximum of the magneto-resistance versus the applied magnetic field.

Figure 10: Temperature dependence of the heat capacity without external magnetic field and under 1 tesla.

Figures:

Figure 1:

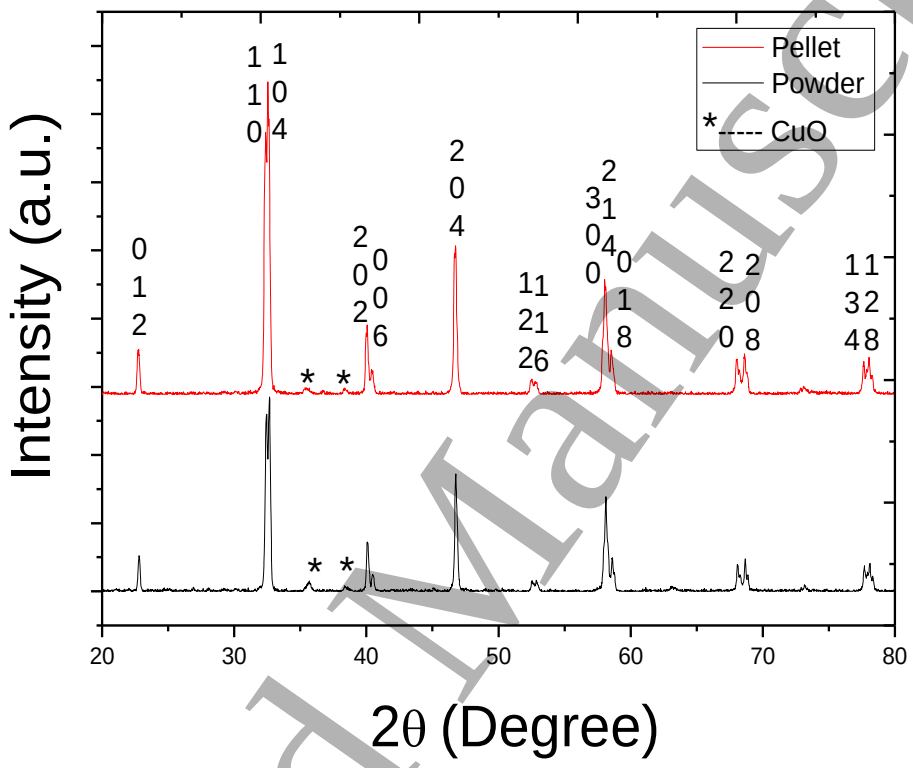

Figure 2 :

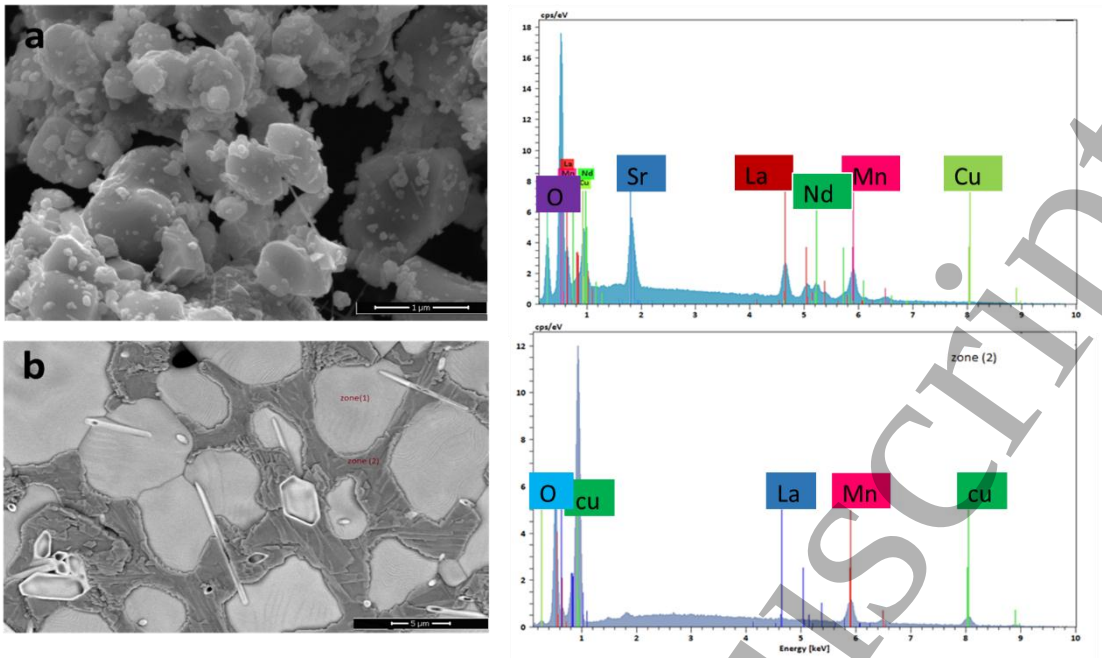

Figure 3:

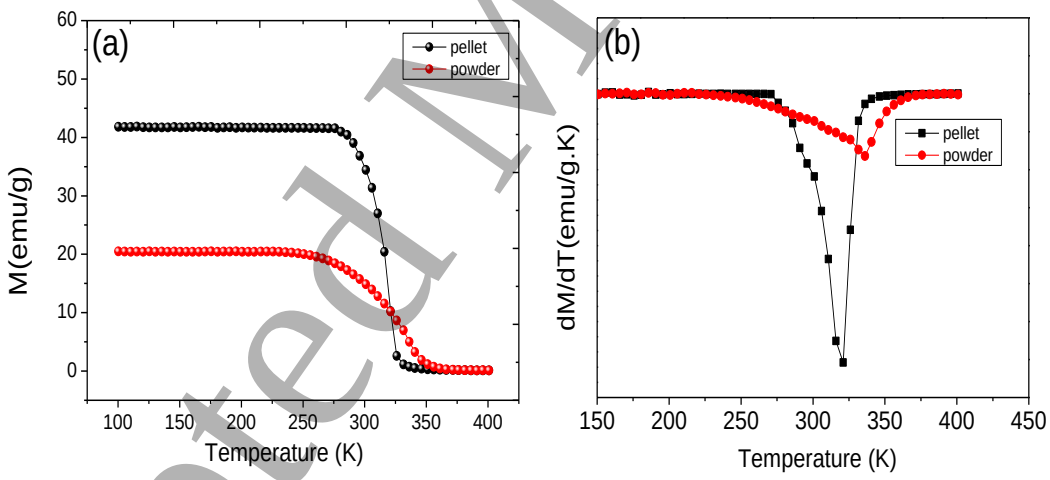

Figure 4

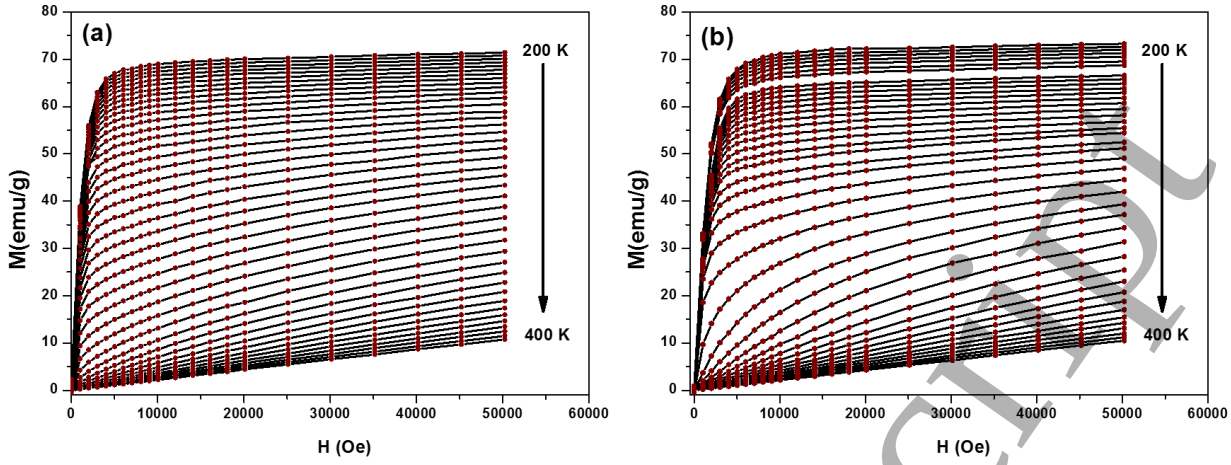

Figure 5:

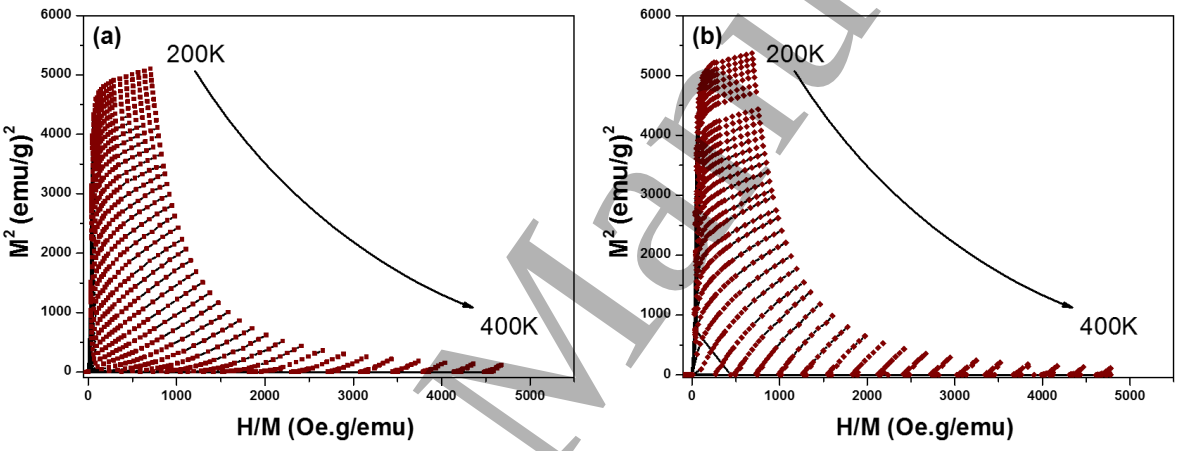

Figure 6:

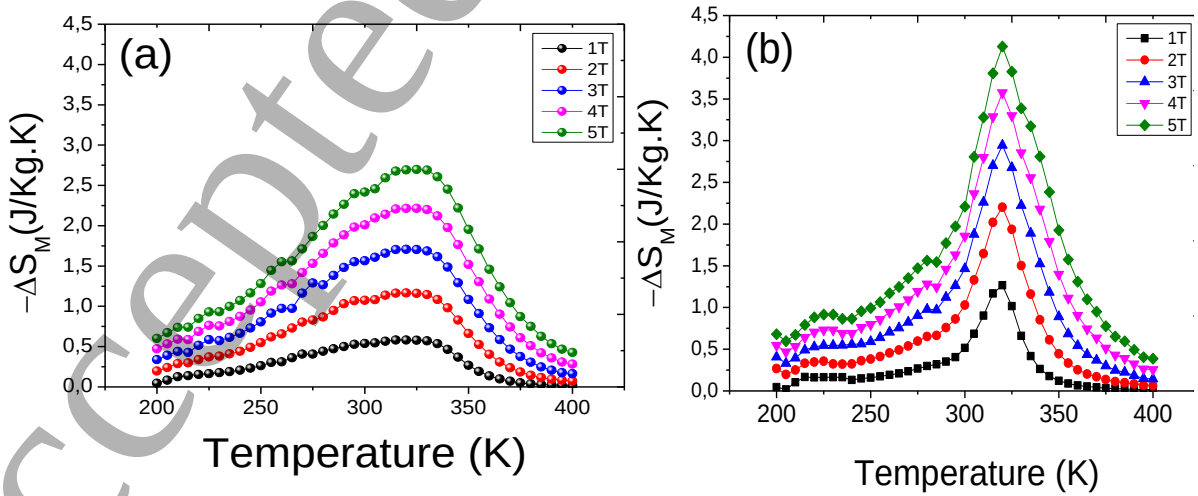

Figure 7

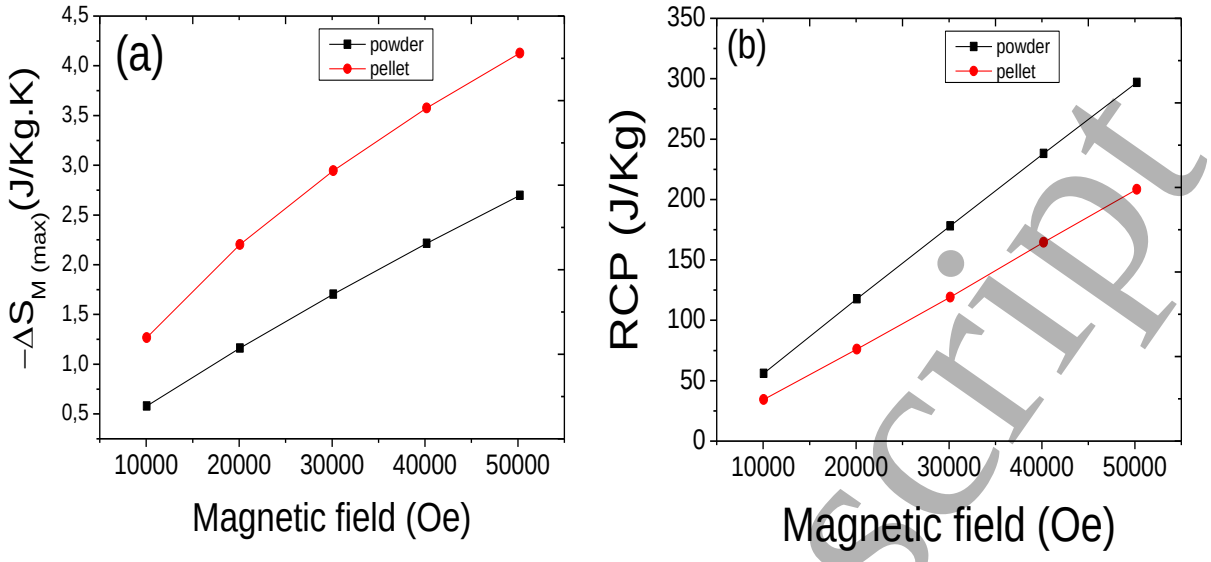

Figure 8:

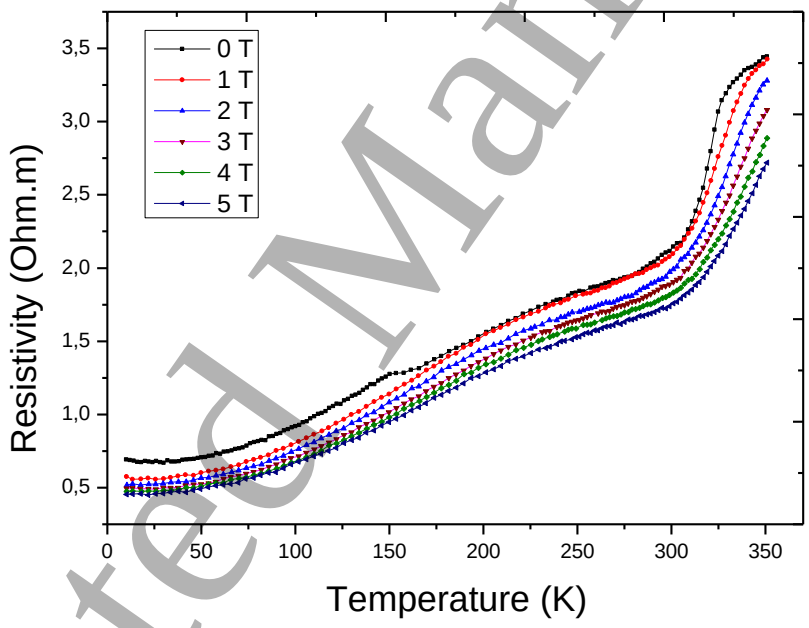

Figure 9 :

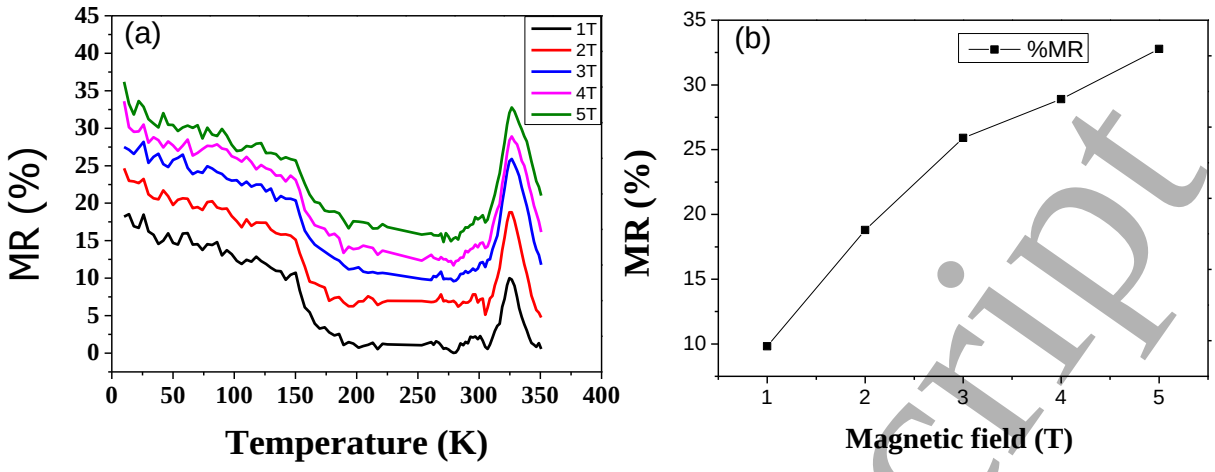

Figure 10

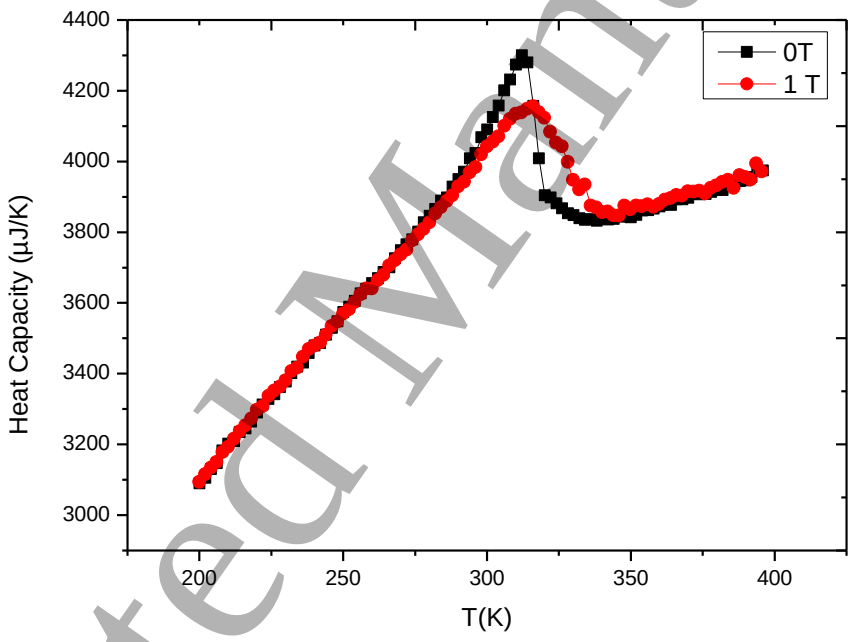

Graphical Abstract:

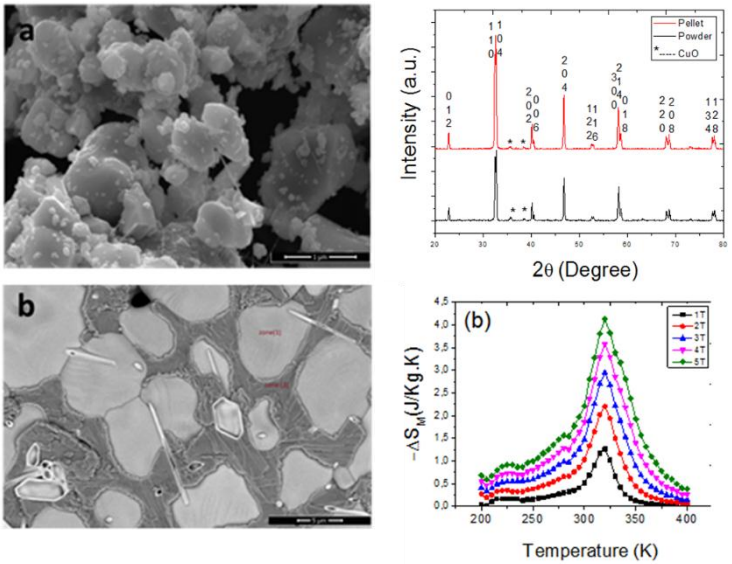

Declarations

Acknowledgment: This work was supported by the MESRSFC (Ministère de l'Enseignement Supérieur, de la Recherche Scientifique et de la Formation des Cadres) in the Framework of the national program PPR under contract no. PPR/2015/57. A. Mahmoud is grateful to the Walloon region for a Beware Fellowship Academia 2015-1, RESIBAT n° 1510399.

Declaration of interests

The authors declare that they have no known competing financial interests or personal relationships that could have appeared to influence the work reported in this paper.